Nox2-derived radicals contribute to neurovascular and behavioral dysfunction in mice overexpressing the amyloid precursor protein

Laibaik Park*, Ping Zhou*, Rose Pitstick†, Carmen Capone*, Josef Anrather*, Erin H. Norris‡, Linda Younkin§, Steven Younkin§, George Carlson†, Bruce S. McEwen‡¶, and Costantino Iadecola*¶

*Division of Neurobiology, Department of Neurology and Neuroscience, Weill Medical College of Cornell University, New York, NY 10065; ‡Harold and Margaret Milliken Hatch Laboratory of Neuroendocrinology, The Rockefeller University, New York, NY 10065; §Mayo Clinic Jacksonville, Jacksonville, FL 32224; and †McLaughlin Research Institute, Great Falls, MT 59405

Contributed by Bruce S. McEwen, December 7, 2007 (sent for review October 23, 2007)

Alterations in cerebrovascular regulation related to vascular oxidative stress have been implicated in the mechanisms of Alzheimer's disease (AD), but their role in the amyloid deposition and cognitive impairment associated with AD remains unclear. We used mice overexpressing the Swedish mutation of the amyloid precursor protein (Tg2576) as a model of AD to examine the role of reactive oxygen species produced by NADPH oxidase in the cerebrovascular alterations, amyloid deposition, and behavioral deficits observed in these mice. We found that 12- to 15-month-old Tg2576 mice lacking the catalytic subunit Nox2 of NADPH oxidase do not develop oxidative stress, cerebrovascular dysfunction, or behavioral deficits. These improvements occurred without reductions in brain amyloid-β peptide (Aβ) levels or amyloid plaques. The findings unveil a previously unrecognized role of Nox2-derived radicals in the behavioral deficits of Tg2576 mice and provide a link between the neurovascular dysfunction and cognitive decline associated with amyloid pathology.

Alzheimer's disease | cerebral blood flow | tg2576

The amyloid-β peptide (Aβ) is central to the pathogenesis of Alzheimer's disease (AD), the most common form of dementia in the elderly (1). Aβ peptides are cleaved from the amyloid precursor protein (APP) by two aspartyl proteases, termed β- and γ-secretases, and form deposits in the brain parenchyma (amyloid plaques) and around blood vessels (amyloid angiopathy) (2). The mechanisms by which Aβ leads to cognitive impairment have not been completely elucidated, although recent evidence suggests that small aggregates of Aβ may be key pathogenic factors by disrupting synaptic function and inducing neuronal death (2).

However, Aβ also exerts powerful effects on cerebral blood vessels (3). *In vitro* and *in vivo* studies have demonstrated that Aβ enhances vasoconstriction, impairs responses to vasodilators, and reduces cerebral blood flow (CBF) (4, 5). In addition, transgenic mice overexpressing APP and Aβ have major alterations in resting CBF and in key cerebrovascular control mechanisms (5–9). For example, the increase in CBF induced by neural activity (functional hyperemia), a response that matches the brain's energy demands with its blood supply, and the ability of cerebral endothelial cells to regulate CBF are profoundly impaired in mice overexpressing APP (7, 10). The vasoconstriction induced by Aβ may underlie the marked reductions in CBF observed in the early stages of AD (11). The harmful cerebrovascular effects of Aβ, in concert with epidemiological and pathological findings linking AD with cerebrovascular diseases (12–16), have suggested that Aβ has deleterious actions both on neurons and cerebral blood vessels, which may act synergistically to induce brain dysfunction in AD (3, 17).

The cerebrovascular alterations observed in mice overexpressing APP are associated with vascular oxidative stress and are counteracted by free radical scavengers (6, 18, 19), implicating reactive oxygen species (ROS) in the dysfunction. A major source of ROS in brain and blood vessels is the superoxide-producing enzyme NADPH oxidase (20). Genetic inactivation of Nox2, one isoform of the catalytic subunit of NADPH oxidase, counteracts the oxidative stress and the vascular dysfunction induced by Aβ, pointing to NADPH oxidase as the source of the ROS (21). However, these studies were performed in 3- to 4-month-old Tg2576 mice, an age when amyloid plaques and behavioral deficits are not yet present (18, 22, 23). Therefore, the contribution of Nox2-derived radicals to the cerebrovascular alterations, amyloid deposition, and behavioral deficits associated with APP overexpression could not be assessed.

We used aged Tg2576 mice lacking Nox2 to determine whether ROS derived from NADPH oxidase contribute to the cerebrovascular dysfunction, amyloid deposition, and behavioral deficits induced by APP overexpression. We found that genetic inactivation of Nox2 reduces oxidative stress and rescues both the vascular and behavioral alterations observed in 12- to 15-month-old Tg2576 mice. These improvements occurred in the absence of a reduction in amyloid plaques. Thus, the cerebrovascular dysfunction induced by Nox2-derived radicals may have a role in the neuronal dysfunction underlying the cognitive impairment in Tg2576 mice.

Results

Nox2 Deletion Rescues the Cerebrovascular Dysfunction in Aged Tg2576 Mice. We studied crosses between Tg2576 mice (22) and mice deficient in the Nox2 catalytic subunit of NADPH oxidase (24). First, we compared young (3- to 4-month-old) and aged (12- to 15-month-old) Tg2576 mice to determine the effects of aging and amyloid deposition on the neurovascular dysfunction. We used a cranial window preparation to examine the increase in CBF evoked in the whisker barrel cortex by mechanical stimulation of the facial whiskers (functional hyperemia) (7). To study the ability of endothelial cells to regulate CBF, we topically applied acetylcholine (ACh), bradykinin, or the calcium ionophore A23187 to the neocortex, a well established approach to test endothelium-dependent relaxation of brain vessels (25). ACh increases CBF by activating endothelial nitric oxide synthase via endothelial muscarinic receptors (26, 27), bradykinin acts through endothelial bradykinin receptors and cyclooxygenase-1 products (28–30), and A23187 increases CBF in a receptor independent manner via cyclooxygenase-1 products (25, 30). Functional hyperemia, and the increase in CBF produced by ACh or bradykinin were attenuated by aging in WT mice, but not in Nox2-null mice (Fig. 1 *A–C*; $P < 0.05$; analysis of variance; $n = 5$ per group), attesting to the

Author contributions: L.P., P.Z., J.A., G.C., B.S.M., and C.I. designed research; L.P., R.P., C.C., L.Y., and S.Y. performed research; P.Z., J.A., E.H.N., L.Y., S.Y., G.C., and B.S.M. contributed new reagents/analytic tools; L.P., S.Y., B.S.M., G.C., and C.I. analyzed data; and L.P., G.C., B.S.M., and C.I. wrote the paper.

The authors declare no conflict of interest.

¶To whom correspondence may be addressed. E-mail: mcewen@rockefeller.edu or coi2001@med.cornell.edu.

This article contains supporting information online at www.pnas.org/cgi/content/full/0711568105/DC1.

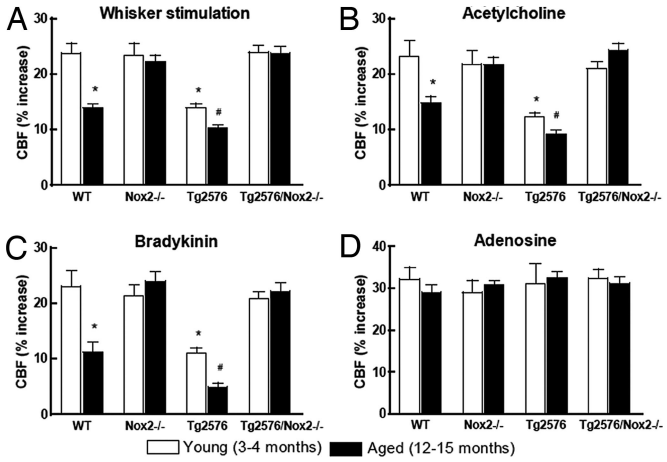

Fig. 1. Nox2 inactivation rescues the cerebrovascular dysfunction in Tg2576 mice. CBF responses to whisker stimulation (*A*) and topical neocortical application of acetylcholine (10 μM) (*B*), bradykinin (50 μM) (*C*), or adenosine (400 μM) (*D*) in young and aged WT, Nox2$^{-/-}$, Tg2576, or Tg2576/Nox2$^{-/-}$ mice. *, $P < 0.05$ from young WT; #, $P < 0.05$ from young Tg2576; analysis of variance and Tukey's test; $n = 5$ per group.

involvement of Nox2-derived ROS in the neurovascular dysfunction of aging (31). Aging did not attenuate the CBF response to A23187 in WT mice [supporting information (SI) Fig. 6*A*]. Functional hyperemia and CBF responses to ACh and bradykinin were attenuated both in young and aged Tg2576 mice, the attenuation being more marked in aged Tg2576 mice (Fig. 1 *A–C*; $P < 0.05$; $n = 5$ per group). However, CBF responses were not reduced in young and aged Tg2576 mice crossed with Nox2-null mice (Tg2576/Nox2$^{-/-}$) (Fig. 1 *A–C*; $P > 0.05$; $n = 5$ per group). The increase in CBF evoked by hypercapnia or by the smooth muscle relaxant adenosine was preserved in all genotypes (Fig. 1*D* and SI Fig. 6*B*; $n = 5$ per group), indicating that smooth muscle reactivity was intact. These observations establish that the cerebrovascular dysfunction induced by APP overexpression is worse in aged Tg2576 mice but that inactivation of Nox2 rescues the dysfunction in full.

Nox2 Deletion Attenuates Oxidative Stress in Aged Tg2576 Mice. Next, we sought to determine whether the rescue of the cerebrovascular alterations observed in aged Tg2576/Nox2$^{-/-}$ mice was related to a reduction in oxidative stress. To this end, we examined ROS production, using hydroethidine microfluorography (21) in WT, Tg2576, and Tg2576/Nox2$^{-/-}$ mice (12–15 months of age). Cell specific markers were used to identify the cell type producing ROS (see *Methods*). In Tg2576 mice, the ROS signal was markedly increased in neurons and endothelial cells (Fig. 2). Although microglia and astrocytes were increased in the brain of Tg2576 mice, these cells were not a major source of ROS (SI Fig. 7). The lack of ROS increase in astrocytes and microglia was not due to the ROS detection technique, because superfusion with the protein kinase C activator phorbol myristate acetate (PMA) was able to increase ROS in these cells (SI Fig. 7*B g–i* and *p–r*). The increase in ROS signal was blocked by the free radical scavenger manganic(I-II)meso-tetrakis(4-benzoic acid) porphyrin (MnTBAP), attesting to the validity of the method (Fig. 2*C*). Superfusion with the NADPH oxidase peptide inhibitor gp91ds-tat, but not its scrambled version, blocked the increase in ROS (Fig. 2*C*). Furthermore, the increased ROS production was not observed in Tg2576/Nox2$^{-/-}$ mice (Fig. 2*C*). Therefore, the rescue of neurovascular dysfunction by Nox2 gene inactivation in Tg2576 mice is associated with reduced vascular and neuronal oxidative stress.

A Free Radical Scavenger or a Peptide Inhibitor of NADPH Oxidase Ameliorates Neurovascular Dysfunction in Aged Tg2576 Mice. In these studies, we examined whether the neurovascular dysfunction ob-

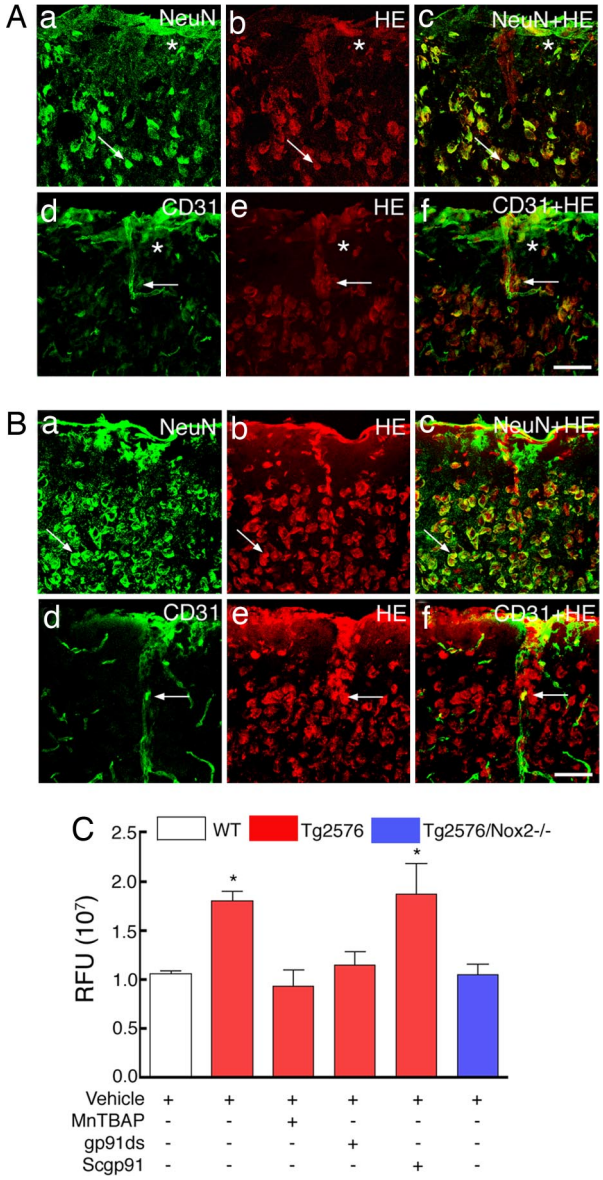

Fig. 2. Nox2 inactivation attenuates neuronal and vascular oxidative stress in 12–15-month-old Tg2576 mice. (*A*) Wild-type mice. Neurons immunolabeled with NeuN (*a*) are colocalized with the ROS (HE) signal (*b*), as shown by the merged image (*c*). Endothelial cells immunolabeled with CD31 (*d*) are also colocalized with the ROS signal (*e* and *f*). (Scale bar: 50 μm.) (*B*) Tg2576 mice. NeuN-positive neurons (*a*) are colocalized with the ROS signal (*b* and *c*). CD31-positive endothelial cells (*d*) are also colocalized with the ROS signal (*e* and *f*). (Scale bar: 50 μm.) (*C*) The increased ROS signal in Tg2576 is attenuated by the ROS scavenger MnTBAP and a NADPH peptide inhibitor (gp91-ds) but not by a scrambled peptide (sgp91ds) or in Tg2576/Nox2$^{-/-}$ crosses. *, $P < 0.05$ from WT; analysis of variance and Tukey's test; $n = 5$ per group.

served in 12- to 15-month-old Tg2576 mice was irreversible or could be ameliorated by agents that counteract oxidative stress. Superfusion of the neocortex with MnTBAP for 30 min did not affect resting CBF (SI Fig. 8*A*; $P > 0.05$; $n = 5$ per group), but it completely reversed the attenuation of the increase in CBF produced by whisker stimulation, ACh, bradykinin, and A23187 (Fig. 3 *A–C* and SI Fig. 8*B*; $P > 0.05$ from young WT mice). MnTBAP did not affect CBF responses to adenosine or hypercapnia (Fig. 3*D* and SI Fig. 8*C*; $P > 0.05$), attesting to the selectivity of the effect. Then, we used the NADPH oxidase peptide inhibitor gp91ds-tat to examine whether NADPH oxidase was the source of the ROS

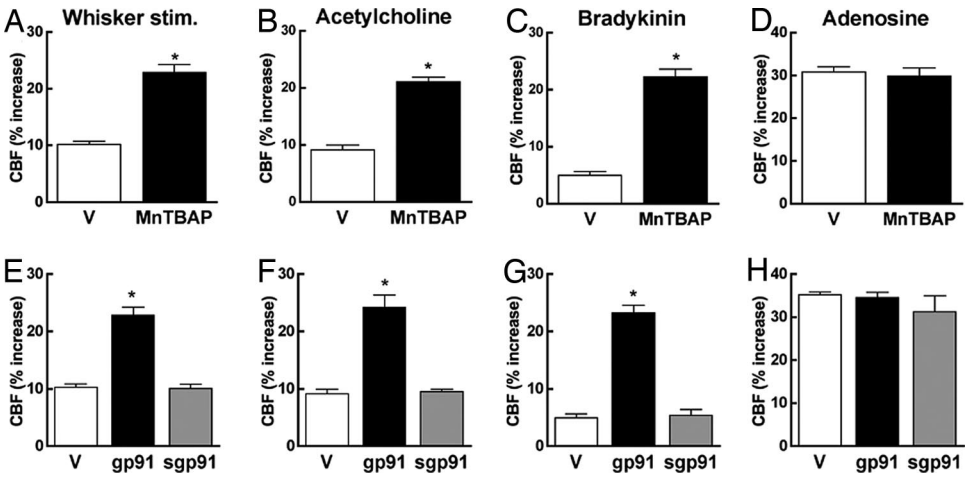

Fig. 3. Short-term application of ROS scavengers counteracts the cerebrovascular dysfunction in 12- to 15-month-old Tg2576 mice. Cerebrovascular responses are rescued by a 30-min neocortical application of MnTBAP (*A–C*) or gp91ds-tat (gp91ds) (*E–G*) but not by a scrambled peptide (sgp91) (*E–G*). Responses to adenosine are not attenuated in Tg2576 mice (*D* and *H*). *, $P < 0.05$ from vehicle; analysis of variance and Tukey's test; $n = 5$ per group. V, vehicle.

mediating the dysfunction. Superfusion with gp91ds-tat, but not its scrambled control, reversed the attenuation in cerebrovascular responses observed in Tg2576 mice (Fig. 3 *E–H* and SI Fig. 8 *D–F*; $P > 0.05$ from young WT mice). Therefore, the neurovascular dysfunction in aged Tg2576 can be corrected by counteracting oxidative stress.

Nox2 Deletion Does Not Affect Plaque Load or Brain Aβ in Aged Tg2576 Mice. To determine whether the attenuation in ROS production and neurovascular dysfunction was related to a reduction in Aβ accumulation in the brain of aged Tg2576/Nox2$^{-/-}$ mice, we measured brain Aβ in the Tg2576 and Tg2576/Nox2$^{-/-}$ mice used in CBF experiments. SDS-soluble and -insoluble $A\beta_{1-40}$ and $A\beta_{1-42}$ levels did not differ between Tg2576 and Tg2576/Nox2$^{-/-}$ mice (Fig. 4 *A* and *B*; $P > 0.05$; $n = 12$ per group). Similarly, plaque number per square millimeter and the area occupied by plaques (plaque load) in neocortex and hippocampus were comparable in Tg2576 and Tg2576/Nox2$^{-/-}$ mice (Fig. 4 *C–F*; $P > 0.05$; $n = 6$ per group). Amyloid angiopathy was occasionally observed in 12-month-old Tg2576 mice, but was more frequent in older mice (SI Fig. 9). Plaque load and brain Aβ levels did not differ between Tg2576 and Tg2576/Nox2$^{-/-}$ mice even at 24 months of age when plaques and brain Aβ levels were more abundant (SI Fig. 10). Therefore, the rescue of the cerebrovascular dysfunction observed in Tg2576/Nox2$^{-/-}$ mice occurs without a reduction in the amyloid burden.

Nox2 Deletion Improves Behavioral Performance in Young and Aged Tg2576 Mice. Finally, we used a two-trial spatial-memory task in a Y maze (32, 33) to determine whether the reduced neurovascular dysfunction and oxidative stress in Tg2576/Nox2$^{-/-}$ mice are associated with improved cognitive performance. We chose this test because it is less stressful and more consistent with the natural behavior of mice than other spatial memory tests, such as the Morris water maze (33), and has been used in experiments involving Tg2576 (34). Furthermore, the Y maze test does not involve learning new rules and takes advantage of the natural tendency of rodents to explore new environments (32). During their first trial (acquisition), mice were allowed to visit two arms of a Y maze, while the third arm was blocked. During the second trial (retrieval) performed 30 min later, access to the closed arm was allowed, so mice were able to explore all three arms. Novel arm entries, time spent in the novel arm, total arm visits, and amount of defecation (an index of anxiety) were recorded. Although young Tg2576 mice showed a preference for the novel arm comparable to that of WT mice, aged Tg2576 mice visited the novel arm less often (Fig. 5*A*; $P < 0.05$, χ^2 test; $n = 10–15$ per group). Furthermore, both young and aged Tg2576 mice spent less time exploring the novel arm than WT or Nox2$^{-/-}$ mice (Fig. 5*B*; $P < 0.05$; analysis of variance). The total number of arm visits and the amount of defecation were increased in Tg2576 mice (Fig. 5 *C* and *D*; $P < 0.05$), reflecting increased locomotor activity and anxiety, respectively. These alterations are consistent with the behavioral deficits reported in Tg2576 mice (34). However, in Tg2576/Nox2$^{-/-}$ mice, novel arm entries and time spent in the novel arm were not reduced (Fig. 5 *A* and *B*; $P > 0.05$ from WT), whereas the increases in total arm visits and

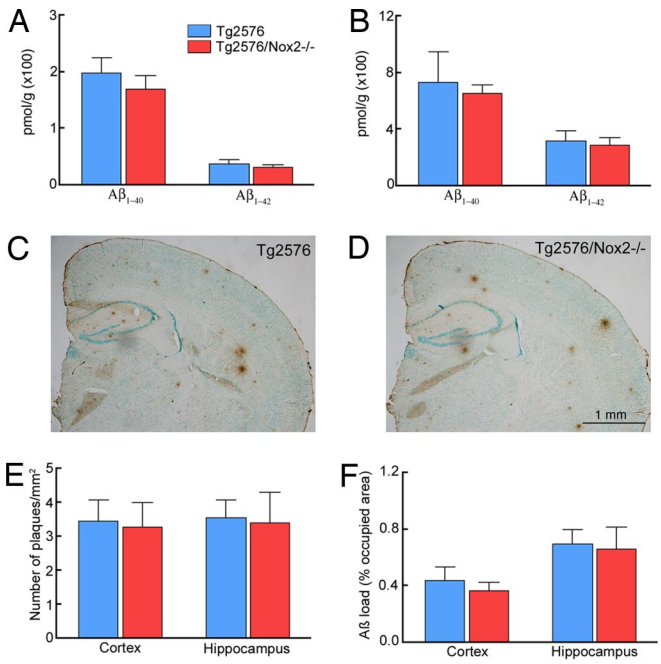

Fig. 4. Brain Aβ and amyloid burden are not reduced in 12- to 15-month-old Tg2576 mice lacking Nox2. (*A* and *B*) SDS-soluble (*A*) and -insoluble (*B*) Aβ are not different in Tg2576 and Tg2576/Nox2$^{-/-}$ mice ($P > 0.05$; analysis of variance and Tukey's test; $n = 12$ per group). (*C* and *D*) The amyloid load is comparable between Tg2576 (*C*) and Tg2576/Nox2$^{-/-}$ mice (*D*). (*E* and *F*) The number of plaques (*E*) and plaque load (*F*) do not differ between Tg2576 and Tg2576/Nox2$^{-/-}$ mice ($P > 0.05$; $n = 6$ per group).

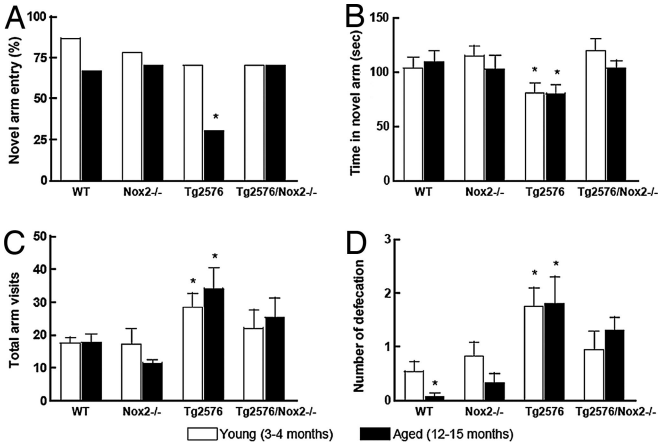

Fig. 5. Nox2 inactivation rescues the behavioral deficits in Tg2576 mice tested in a Y maze. The reduction in novel arm entry (*A*), time spent in the novel arm (*B*), and the increase in total arm visits (*C*) and defecation (*D*) observed in Tg2576 mice are not seen in Tg2576/Nox2$^{-/-}$ mice. *, $P < 0.05$, χ^2 test in *A* and analysis of variance and the Newman–Keul test in *B–D*; $n = 10–15$ per group.

defecation were attenuated (Fig. 5 *C* and *D*; $P > 0.05$ from WT). Therefore, Tg2576 mice lacking Nox2 are protected from the behavioral dysfunction induced by APP overexpression.

Discussion

We have demonstrated that Tg2576 mice have an age-dependent dysfunction in the mechanisms regulating CBF associated with oxidative stress and behavioral deficits. Oxidative stress, neurovascular dysfunction, and behavioral deficits are not present in aged Tg2576 mice lacking Nox2, implicating Nox2-derived ROS in the mechanisms of the dysfunction. The improvement in CBF regulation and behavior conferred by Nox2 inactivation occurs without reductions of brain Aβ levels and amyloid deposition. Furthermore, the cerebrovascular dysfunction in aged Tg2576 mice can be counteracted by short-term treatment with a ROS scavenger or a peptide inhibitor of NADPH oxidase. These observations unveil a key role of Nox2 derived ROS in the neurovascular dysfunction and behavioral deficits induced by APP overexpression and Aβ.

Studies have demonstrated that APP overexpressing mice have structural and functional abnormalities in cerebral blood vessels, some of which are related to oxidative stress (3, 17). However, most studies were conducted in mice at an age when the amyloid deposition and behavioral deficits were not present (6). Although these investigations provided evidence that Aβ-induced vascular dysfunction is an early pathogenic event and is mediated by Nox2-derived ROS (21), they were unable to provide insight into the relationships among neurovascular dysfunction, amyloid deposition, and behavioral deficits. Other investigators examined the effect of APP overexpression on the morphology of cerebral arteries and cerebral blood volume in mice at an age when amyloid deposition was thought to be present (35, 36). However, these investigations did not attempt to determine the mechanisms of the effect and its impact on the amyloid deposition and behavioral deficits. Therefore, the evidence provided here establishes a link between Nox2-dependent oxidative stress, neurovascular dysfunction, and behavioral deficits in Tg2576 mice.

The vascular responses to whisker stimulation, ACh, and bradykinin were attenuated more in aged than in young Tg2576 mice. This effect cannot result from a generalized vasoparalysis, because the CBF responses to adenosine were not attenuated in aged Tg2576 mice, suggesting that smooth muscle function was preserved. Considering that aging attenuates CBF responses also in WT mice via Nox2-derived ROS (31), it is more likely that aging and the associated increase in brain Aβ levels acted in concert to enhance oxidative stress and the vascular dysfunction. The observation that vascular responses are normalized in Tg2576 mice lacking Nox2 suggests that Nox2-dependent ROS production is the final common pathway for the vascular alterations induced both by aging and Aβ. However, a contribution from the alterations in smooth muscle contractility induced by myocardin in Tg2576 mice cannot be ruled out (37).

One of the key findings of the present study is that restoration of cerebrovascular function in Tg2576/Nox2$^{-/-}$ mice is associated with improvement of the behavioral deficits. Studies have reported that attenuation of oxidative or nitrosative stress ameliorates the cognitive impairment in mice overexpressing APP, but the improvement was usually associated with a reduction in amyloid plaques (38–40). However, in the present study, the behavioral improvement occurred without reductions in brain Aβ levels or amyloid burden. Thus, amyloid deposition can be dissociated from the behavioral deficits. This finding has two major implications. First, it provides further evidence that in mouse models as in AD amyloid plaques do not predict the brain dysfunction underlying the cognitive deficits (41). Increasing evidence suggests that smaller Aβ aggregates are potent mediators of synaptotoxicity and neuronal death and best correlate with behavioral deficits (2). Second, this finding suggests that Nox2-derived radicals, although contributing to the neurovascular dysfunction and behavioral deficits induced by APP overexpression, do not have a role in Aβ processing and amyloid plaque formation. In contrast, enhancing mitochondrial ROS production by inactivation of one allele of mitochondrial superoxide dismutase increases the amyloid burden in mice overexpressing human APP (42, 43). Conversely, the free radical scavenger curcumin reduced amyloid load in mice overexpressing APP (40, 44). Thus, not all sources of ROS contribute equally to plaque formation. These observations, collectively, suggest a previously unrecognized specificity in the sources of ROS promoting Aβ deposition. However, our findings do not provide insights into the roles of Nox2-derived ROS in the amyloid angiopathy and its contribution to the cerebrovascular and behavioral dysfunction observed in Tg2576 mice.

An important question concerns whether there is a causal link between the rescue of vascular function and the enhancement in behavioral performance observed in Tg2576 mice lacking Nox2. Although Nox2 inactivation reduces neuronal oxidative stress, which may improve neuronal function and behavior, our data suggest that vascular responses mediated by direct actions on cerebral blood vessels also are rescued. Thus, the restoration of responses to the endothelium-dependent vasodilators ACh, bradykinin, and A23187 cannot be attributed to an improvement in neuronal function because these responses are independent of neurons (25). Inasmuch as vascular dysregulation limits the supply of vital nutrients to the working brain and increases its susceptibility to injury, the improvement in vascular function in Tg2576 mice after Nox2 inactivation should ameliorate neuronal function, which is compromised by oxidative stress. Therefore, it is likely that improvement of both vascular and neuronal function contribute to the improvement of behavioral performance.

We have also observed that short-term administration of a free radical scavenger or of a NADPH oxidase peptide inhibitor counteracts oxidative stress and neurovascular dysfunction in aged Tg2576 mice. This finding suggests that the vascular dysfunction is reversible, even in aged mice with long-lasting oxidative stress, amyloid deposition, and behavioral deficits. Therefore, vascular oxidative stress does not produce permanent vascular damage, but it induces a dysfunctional state that can be rescued by transient antioxidant treatment. Treatment with agents that scavenge ROS have been reported to ameliorate behavioral deficits in Tg2576 mice (40). Our data suggest that improvement of vascular function may have a role in the improvement in cognition as well.

In conclusion, we have demonstrated that Nox2 inactivation reduces vascular and neuronal oxidative stress, improves the neurovascular dysfunction, and ameliorates the behavioral deficits in aged Tg2576 mice. These improvements are independent of reductions of brain Aβ levels and amyloid burden. Furthermore, transient antioxidant treatment ameliorates the vascular dysfunction, indicating that the deleterious effects of oxidative stress on brain vessels are not permanent and are amenable to reversal by therapeutic interventions. The findings demonstrate that Nox2 derived ROS are involved both in the vascular dysfunction induced by APP overexpression and in the associated behavioral decline. Vascular and behavioral improvements take place without a reduction in brain Aβ load and amyloid plaques, indicating that Nox2-derived ROS are not involved in the mechanisms of plaque formation, and suggesting an unforeseen specificity in the ROS sources involved in Aβ processing and deposition.

Methods

Mice. All procedures were approved by the Institutional Animal Care and Use Committee of Weill Cornell Medical College. All experiments were performed in male mice of ages ranging from 3 to 15 months. Methods for crossing APP mice with Nox2$^{-/-}$ mice were identical to those described in ref. 21. Briefly, breeder pairs of B6.129-*Cybb*^{tm1Din}/J mice lacking the Nox2 subunit of NADPH oxidase (24) were maintained by brother (hemizgous for the null allele)–sister (homozygous null) matings (21). The Tg2576 transgenic line overexpresses the Swedish mutant (K670N M671I) human APP$_{695}$ driven by hamster prion protein promoter (22). The Tg2576 transgene array was maintained on a mixed B6/SJL background and on the inbred 129S6 background (7). PCR was used for genotyping the APP transgene array as described in ref. 7. To produce Tg2576 mice with or without Nox2, Nox2$^{-/-}$ females were crossed to Tg2576 males; because the gene encoding Nox2 (*Cybb*) is on the X chromosome, male offspring do not express Nox2. To produce Tg2576-positive or -negative mice expressing Nox2, C57BL/6J females were crossed to Tg2576 males; only male offspring were used. CBF results did not differ between the offspring of B6/SJL-Tg2576 or 129S6.Tg2576 males.

General Surgical Procedures. Mice were anesthetized with isoflurane (maintenance 2%), intubated, and artificially ventilated (SAR-830; CWE) (6, 7, 21). The femoral vessels were cannulated for recording of arterial pressure and blood sample collection. Rectal temperature was maintained at 37°C. After surgery, anesthesia was maintained with urethane (750 mg/kg; i.p.) and chloralose (50 mg/kg; i.p.) (6, 7, 21).

CBF and Cerebrovascular Reactivity. A craniotomy (2 × 2 mm) was performed to expose the somatosensory cortex, the dura was removed, and the site was superfused with a modified Ringer solution (37°C; pH 7.3–7.4) (6, 7, 21). CBF was monitored at the site of superfusion with a laser–Doppler probe (Vasamedic) positioned stereotaxically on the brain surface and connected to a computer. CBF was expressed as percentage increase relative to the resting level.

Detection of Reactive Oxygen Species. ROS production was assessed by using hydroethidine (HE) as a marker (21). HE (2 μM; Molecular Probes) was superfused on the somatosensory cortex for 60 min (21). Sections (20 μm thick) were cut through cortex underlying the cranial window, using a cryostat; collected at 100-μm intervals; and examined under a fluorescence microscope (Nikon). Images were acquired with a digital camera (Coolsnap; Roper Scientific), using the same settings in all cases. The analysis was performed in a blinded fashion, using IPLab software (Scanalytics). Fluorescent intensities of all sections (15–20 per animal) were expressed as relative fluorescence units (RFU) (21).

Immunocytochemistry and Confocal Microscopy. Mice were anesthetized with 5% isoflurane and perfused transcardially with 4% paraformaldehyde (PFA). The brain region underlying the cranial window was sectioned in a cryostat (14 μm thick). To identify HE-positive cells, sections were processed for immunohistochemistry with NeuN (1:100; Sigma), GFAP (1:1,000; Sigma), CD31 (1:100; BD Biosciences), or CD11b (1:100; BD Parmingen). Sections were then incubated with cyanine dye (Cy5)-conjugated goat anti-mouse IgG (for NeuN, GFAP, and CD11b; Jackson ImmunoResearch) and goat anti-rat IgG (for CD31; Jackson ImmunoResearch) secondary antibodies. The specificity of the labeling was established by omitting the primary antibody or by preabsorption with the antigen. The images were sequentially acquired by using a confocal laser-scanning microscope (Leica).

Measurement of Aβ. Aβ was measured by using an ELISA-based assay, as described in refs. 6, 7, and 21. Briefly, the left hemispheres from the mice used for CBF studies were sonicated in 1% SDS with protease inhibitors and centrifuged. The supernatant contained SDS-soluble Aβ peptides. The pellet was sonicated in 70% formic acid and centrifuged as above. The formic acid extract was neutralized by a 1:20 dilution into 1 M Tris phosphate buffer (pH 8.0). Aβ_{1-40} and Aβ_{1-42} concentrations (picomoles per gram of brain tissue) were determined in supernatant (SDS-soluble) and the formic acid extract of the pellet (SDS-insoluble), using the BAN-50/BA-27 and BAN-50/BC005 sandwich ELISA as described (6, 7, 21).

Determination of Aβ Load. Aβ load was determined as described in ref. 45. Briefly, the right hemisphere of Tg2576 and Tg2576/Nox2$^{-/-}$ mice used for CBF studies (n = 5 per group) was postfixed in 4% PFA. Coronal sections (20 μM thick) were cut in a cryostat at 400-μm intervals from a region located 1.94 to −3.28 mm from bregma. This region includes the cortex underlying the cranial window. Ten sets of 13–14 sections were collected. One of the sets was randomly selected for immunocytochemistry, using an Aβ antibody (4G8; Sigma). Grayscale images (magnification: ×1) of the cortex and hippocampus were digitized with a camera (Q Imaging; Barnaby). The number of plaques per square millimeter were manually counted in the cortex and hippocampus. The Aβ load was determined in a blinded manner from the area occupied by the plaques relative to the total area of cortex or hippocampus, using National Institutes of Health Image software.

Behavioral Assessment by the Y Maze. Behavioral assessment was performed by using the Y maze as described in ref. 33. Briefly, the Y maze consisted of three identical arms made of transparent plastic joined in the middle to form a ''Y'' (20 cm high, 10 cm wide, and 30 cm long). The mice were handled daily and allowed to acclimate to the apparatus for a week before testing. Mice were placed into one of the arms of the maze (start arm) and allowed to explore only two of the arms for 5 min (training trial). The third arm, which remained closed, was randomly chosen in each trial. The closed arm was opened in the test trial, serving as the novel arm. After a 30-min intertrial interval, the mice were returned to the same start arm and were allowed to explore all three arms for 5 min (test trial). Sessions were video recorded and replayed for determination of the parameters of interest by an observer blinded to the genotype of the mice.

Experimental Protocol. CBF recordings were started after arterial pressure and blood gases were in a steady state (SI Tables 1–3).

Functional hyperemia and CBF responses to ACh, bradykinin, A23187, and adenosine. For testing functional hyperemia, the increase in CBF produced by gently stroking the whiskers for 60 sec with a cotton-tipped applicator was recorded. ACh (10 μM; Sigma), bradykinin (50 μM; Sigma), or the calcium ionophore A23187 (3 μM; Sigma) was topically superfused for 3–5 min, and the evoked CBF increase was recorded. The CBF response to adenosine (400 μM; Sigma) was also tested. The increase in CBF induced by hypercapnia (pCO_2 to 50–60 mmHg) was examined by introducing 5% CO_2 in the circuit of ventilator.

Effect of MnTBAP. Responses to functional hyperemia, ACh, bradykinin, A23187, adenosine, and hypercapnia were tested before and after superfusion of the cranial window with the ROS scavenger MnTBAP for 30 min (100 μM; Porphyrin Products).

Effect of gp91ds-tat. As described in ref. 21, the NADPH oxidase assembly peptide inhibitor gp91ds-tat (YGRKKRRQRRRCSTRIRRQL-NH_2) and its scrambled control (sgp91ds-tat) (YGRKKRRQRRRCLRITRQSR-NH_2) (Bio·Synthesis) were studied (46). Cerebrovascular responses were assessed before and 30–40 min after superfusion of gp91ds-tat (1 μM) or sgp91ds-tat (1 μM).

Effects of MnTBAP, gp91ds-tat, and PMA on ROS production. The cranial window was superfused with Ringer's solution, containing HE (2 μM) alone (vehicle) for 60 min or for 30 min followed by HE plus MnTBAP (100 μM), gp91ds-tat (1 μM), or scrambled control peptide (1 μM) for another 30 min. In aged Tg2576 mice, the effect of PMA (5 μM; Sigma) was assessed to test the ability of astrocytes or microglia to generate ROS. At the end of superfusion, brains were removed and processed for ROS assessment.

Data Analysis. Data are expressed as means ± SEM. Two-group comparisons were analyzed by the two-tailed t test. Multiple comparisons were evaluated by the analysis of variance and Tukey's test or the Newman–Keul test. Differences in novel arm entries were analyzed by the χ^2 test (X^2). Differences were considered statistically significant for $P < 0.05$.

ACKNOWLEDGMENTS. This work was supported by National Institutes of Health Grant NS37853.

1. Kelley BJ, Petersen RC (2007) Alzheimer's disease and mild cognitive impairment. *Neurol Clin* 25:577–609.
2. Haass C, Selkoe DJ (2007) Soluble protein oligomers in neurodegeneration: lessons from the Alzheimer's amyloid beta-peptide. *Nat Rev Mol Cell Biol* 8:101–112.
3. Iadecola C (2004) Neurovascular regulation in the normal brain and in Alzheimer's disease. *Nat Rev Neurosci* 5:347–360.
4. Thomas T, Thomas G, McLendon C, Sutton T, Mullan M (1996) β-Amyloid-mediated vasoactivity and vascular endothelial damage. *Nature* 380:168–171.
5. Niwa K, *et al.* (2001) Aβ-peptides enhance vasoconstriction in cerebral circulation. *Am J Physiol Heart Circ Physiol* 281:H2417–H2424.
6. Iadecola C, *et al.* (1999) SOD1 rescues cerebral endothelial dysfunction in mice overexpressing amyloid precursor protein. *Nat Neurosci* 2:157–161.
7. Niwa K, *et al.* (2000) Aβ 1–40-related reduction in functional hyperemia in mouse neocortex during somatosensory activation. *Proc Natl Acad Sci USA* 97:9735–9740.
8. Niwa K, *et al.* (2002) Cerebrovascular autoregulation is profoundly impaired in mice overexpressing amyloid precursor protein. *Am J Physiol Heart Circ Physiol* 283:H315–H323.
9. Niwa K, Kazama K, Younkin SG, Carlson GA, Iadecola C (2002) Alterations in Cerebral Blood Flow and Glucose Utilization in Mice Overexpressing the Amyloid Precursor Protein. *Neurobiol Dis* 9:61–68.
10. Takano T, Han X, Deane R, Zlokovic B, Nedergaard M (2007) Two-photon imaging of astrocytic Ca^{2+} signaling and the microvasculature in experimental mice models of Alzheimer's disease. *Ann NY Acad Sci* 1097:40–50.
11. Johnson KA, Albert MS (2000) Perfusion abnormalities in prodromal AD. *Neurobiol Aging* 21:289–292.
12. Beach TG, *et al.* (2007) Circle of Willis atherosclerosis: association with Alzheimer's disease, neuritic plaques and neurofibrillary tangles. *Acta Neuropathol (Berlin)* 113:13–21.
13. Snowdon DA, *et al.* (1997) Brain infarction and the clinical expression of Alzheimer disease. The Nun Study. *J Am Med Assoc* 277:813–817.
14. Skoog I, Gustafson D (2002) Hypertension and related factors in the etiology of Alzheimer's disease. *Ann NY Acad Sci* 977:29–36.
15. Ruitenberg A, *et al.* (2005) Cerebral hypoperfusion and clinical onset of dementia: The Rotterdam Study. *Ann Neurol* 57:789–794.
16. Silvestrini M, *et al.* (2006) Cerebrovascular reactivity and cognitive decline in patients with Alzheimer disease. *Stroke* 37:1010–1015.
17. Zlokovic BV (2005) Neurovascular mechanisms of Alzheimer's neurodegeneration. *Trends Neurosci* 28:202–208.
18. Park L, *et al.* (2004) Aβ-induced vascular oxidative stress and attenuation of functional hyperemia in mouse somatosensory cortex. *J Cereb Blood Flow Metab* 24:334–342.
19. Tong XK, Nicolakakis N, Kocharyan A, Hamel E (2005) Vascular remodeling versus amyloid beta-induced oxidative stress in the cerebrovascular dysfunctions associated with Alzheimer's disease. *J Neurosci* 25:11165–11174.
20. Bedard K, Krause KH (2007) The NOX family of ROS-generating NADPH oxidases: Physiology and pathophysiology. *Physiol Rev* 87:245–313.
21. Park L, *et al.* (2005) NADPH oxidase-derived reactive oxygen species mediate the cerebrovascular dysfunction induced by the amyloid β peptide. *J Neurosci* 25:1769–1777.
22. Hsiao K, *et al.* (1996) Correlative memory deficits, Aβ elevation, and amyloid plaques in transgenic mice. *Science* 274:99–102.
23. Kawarabayashi T, *et al.* (2001) Age-dependent changes in brain CSF, plasma amyloid (beta) protein in the Tg2576 transgenic mouse model of Alzheimer's disease. *J Neurosci* 21:372–381.
24. Pollock JD, *et al.* (1995) Mouse model of X-linked chronic granulomatous disease, an inherited defect in phagocyte superoxide production. *Nat Genet* 9:202–209.
25. Faraci FM, Heistad DD (1998) Regulation of the cerebral circulation: Role of endothelium and potassium channels. *Physiol Rev* 78:53–97.
26. Rosenblum WI, McDonald M, Wormley B (1989) Calcium ionophore and acetylcholine dilate arterioles on the mouse brain by different mechanisms. *Stroke* 20:1391–1395.
27. Sobey CG, Faraci FM (1997) Effects of a novel inhibitor of guanylyl cyclase on dilator responses of mouse cerebral arterioles. *Stroke* 28:837–843.
28. Sobey CG, Heistad DD, Faraci FM (1997) Mechanisms of bradykinin-induced cerebral vasodilatation in rats. Evidence that reactive oxygen species activate K+ channels. *Stroke* 28:2290–2294.
29. Mayhan WG (1996) Role of activation of bradykinin B2 receptors in disruption of the blood–brain barrier during acute hypertension. *Brain Res* 738:337–341.
30. Niwa K, Haensel C, Ross ME, Iadecola C (2001) Cyclooxygenase-1 participates in selected vasodilator responses of the cerebral circulation. *Circ Res* 88:600–608.
31. Park L, Anrather J, Girouard H, Zhou P, Iadecola C (2007) Nox2-derived reactive oxygen species mediate neurovascular dysregulation in the aging mouse brain. *J Cereb Blood Flow Metab* 27:1908–1918.
32. Dellu F, Contarino A, Simon H, Koob GF, Gold LH (2000) Genetic differences in response to novelty and spatial memory using a two-trial recognition task in mice. *Neurobiol Learn Mem* 73:31–48.
33. Sarnyai Z, *et al.* (2000) Impaired hippocampal-dependent learning and functional abnormalities in the hippocampus in mice lacking serotonin(1A) receptors. *Proc Natl Acad Sci USA* 97:14731–14736.
34. King DL, Arendash GW (2002) Behavioral characterization of the Tg2576 transgenic model of Alzheimer's disease through 19 months. *Physiol Behav* 75:627–642.
35. Beckmann N, *et al.* (2003) Age-dependent cerebrovascular abnormalities and blood flow disturbances in APP23 mice modeling Alzheimer's disease. *J Neurosci* 23:8453–8459.
36. Mueggler T, *et al.* (2003) Age-dependent impairment of somatosensory response in the amyloid precursor protein 23 transgenic mouse model of Alzheimer's disease. *J Neurosci* 22:7218–7224.
37. Chow N, *et al.* (2007) Serum response factor and myocardin mediate arterial hypercontractility and cerebral blood flow dysregulation in Alzheimer's phenotype. *Proc Natl Acad Sci USA* 104:823–828.
38. Nathan C, *et al.* (2005) Protection from Alzheimer's-like disease in the mouse by genetic ablation of inducible nitric oxide synthase. *J Exp Med* 202:1163–1169.
39. Liang X, *et al.* (2005) Deletion of the prostaglandin E2 EP2 receptor reduces oxidative damage and amyloid burden in a model of Alzheimer's disease. *J Neurosci* 25:10180–10187.
40. Cole GM, *et al.* (2004) NSAID and antioxidant prevention of Alzheimer's disease: Lessons from *in vitro* and animal models. *Ann N Y Acad Sci* 1035:68–84.
41. Holcomb LA, *et al.* (1999) Behavioral changes in transgenic mice expressing both amyloid precursor protein and presenilin-1 mutations: Lack of association with amyloid deposits. *Behav Genet* 29:177–185.
42. Esposito L, *et al.* (2006) Reduction in mitochondrial superoxide dismutase modulates Alzheimer's disease-like pathology and accelerates the onset of behavioral changes in human amyloid precursor protein transgenic mice. *J Neurosci* 26:5167–5179.
43. Li F, *et al.* (2004) Increased plaque burden in brains of APP mutant MnSOD heterozygous knockout mice. *J Neurochem* 89:1308–1312.
44. Lim GP, *et al.* (2001) The curry spice curcumin reduces oxidative damage and amyloid pathology in an Alzheimer transgenic mouse. *J Neurosci* 21:8370–8377.
45. Bussiere T, *et al.* (2002) Stereologic assessment of the total cortical volume occupied by amyloid deposits and its relationship with cognitive status in aging and Alzheimer's disease. *Neuroscience* 112:75–91.
46. Rey FE, Cifuentes ME, Kiarash A, Quinn MT, Pagano PJ (2001) Novel competitive inhibitor of NAD (P)H oxidase assembly attenuates vascular O (2)(-) and systolic blood pressure in mice. *Circ Res* 89:408–414.